

Absence of temperature dependence of the valence-band spectrum of Co_2MnSi

K. Miyamoto,¹ A. Kimura,² Y. Miura,³ M. Shirai,³ M. Ye,² Y. Cui,¹ K. Shimada,¹ H. Namatame,¹ M. Taniguchi,^{1,2} Y. Takeda,⁴ Y. Saitoh,⁴ E. Ikenaga,⁵ S. Ueda,⁶ K. Kobayashi,⁶ and T. Kanomata⁷

¹Hiroshima Synchrotron Radiation Center, Hiroshima University, 2-313 Kagamiyama, Higashi-Hiroshima 739-0046, Japan

²Graduate School of Science, Hiroshima University, 1-3-1 Kagamiyama, Higashi-Hiroshima 739-8526, Japan

³Research Institute of Electrical Communication, Tohoku University, Katahira 2-1-1, Aoba-ku, Sendai 980-8577, Japan

⁴Japan Atomic Energy Agency/SPring-8, Sayo, Hyogo 679-5198, Japan

⁵Japan Synchrotron Radiation Research Institute/SPring-8, Sayo, Hyogo 679-5198, Japan

⁶NIMS Beamline Station at SPring-8, National Institute for Materials Science, Sayo, Hyogo 679-5148, Japan

⁷Faculty of Engineering, Tohoku Gakuin University, Tagajo, Miyagi 985-8537, Japan

(Received 27 October 2008; revised manuscript received 20 January 2009; published 23 March 2009)

Valence-band electronic structure of Co_2MnSi has been revealed by photoelectron spectroscopy utilizing hard x-ray synchrotron radiation. We have obtained a good correspondence between experimental valence-band spectra and theoretical density of states calculated with generalized gradient approximation. However, no distinct temperature dependence has been observed for the experimental valence band, which requires re-examination of the explanation based on the dynamical mean-field theory for the rapid decrease in tunneling magnetoresistance ratio with increasing temperature.

DOI: [10.1103/PhysRevB.79.100405](https://doi.org/10.1103/PhysRevB.79.100405)

PACS number(s): 75.50.Cc, 79.60.-i, 71.20.Lp

Recently, spintronics exploiting both charge and spin degrees of freedom has attracted great attention due to the potential for developing advanced functional nanodevices with much less consuming power. In particular, magnetoresistive random access memory (MRAM) composed of tunneling magnetoresistance (TMR) devices is expected as a new non-volatile random access memory with ultra-high density and high clock frequency. Among several materials, half-metallic ferromagnets are the most promising materials for TMR devices. In half-metallic ferromagnets, the density of states (DOS) in one spin direction crosses the Fermi level (E_F) and the DOS in another spin direction shows a semiconducting gap at E_F . Therefore, the conduction-electron spin is 100% polarized and the magnitude of magnetoresistance (MR) could be very large.^{1,2} Although first-principles calculations have predicted many half-metallic ferromagnets, most of them need to be verified by experiments. Among the predicted half-metallic ferromagnets, a full Heusler-type alloy such as Co_2MnSi with $L2_1$ structure is regarded as one of the most promising candidates for a high efficiency TMR device.^{3,4} It shows a Curie temperature sufficiently above room temperature (RT) ($T_C > 900$ K) and large magnetization ($M = 5 \mu_B/\text{formula unit}$).⁵ Large MR ratio (570% at 2 K) has been reported for $\text{Co}_2\text{MnSi-Al}_2\text{O}_3$ -based tunneling magnetic junction. Although the magnitude of the magnetization is almost the same as that at low temperature, the MR ratio decreases down to 67% at RT.⁶ Since the significant reduction in MR ratio with temperature in Co_2MnSi can be strongly related to the reduced electron-spin polarization at E_F , knowledge of electronic states at finite temperatures is quite important. Recently, Chioncel *et al.*⁷ theoretically investigated the effect of electronic correlation at finite temperature utilizing the dynamical mean-field theory (DMFT). In their reports, they suggest that a nonquasiparticle state is formed in the minority-spin state near E_F , promoting the growth of minority-spin DOS in the energy-gap region with increasing temperature.⁷ Although several efforts have been made to determine the electronic structure of bulk and films

of Co_2MnSi by means of photoelectron spectroscopy,⁸⁻¹⁰ no experimental confirmation on the temperature dependence has been provided so far.

Photoemission spectroscopy is a powerful tool for direct observation of the electronic band structure in solids. In general, conventional photoemission spectroscopy in the electron kinetic-energy range of 50–100 eV is quite surface sensitive due to the short electron mean free path of $\sim 5 \text{ \AA}$,¹¹ which roughly corresponds to one unit cell of Co_2MnSi ($\sim 5.65 \text{ \AA}$).¹²⁻¹⁴ The electronic states at surface are strongly reflected in the photoemission spectra, which makes it difficult to examine the bulk-derived electronic states. Although one can extend the probing depth longer than 15 \AA with soft and hard x-ray photons, it was quite difficult to measure valence-band photoelectron spectra above 3 keV due to significantly reduced photoionization cross sections.¹⁵⁻¹⁷ Recently, the third generation synchrotron radiation source with a very low emittance electron beam can well compensate for the diminished cross section and has enabled us to perform soft and hard x-ray photoemission spectroscopies with high-energy resolution.¹⁵ In this Rapid Communication, by means of the soft and hard x-ray photoemission spectroscopies, we clarify the temperature dependence of electronic structures for Co_2MnSi in a condition with suppressed surface contribution.

Polycrystalline Co_2MnSi was prepared by the repeated melting of the appropriate quantities of the constituent elements, namely, 99.9% pure Co, 99.99% pure Mn, and 99.999% pure Si, in an argon arc furnace. Subsequently the sample was sealed in the evacuated double silica tubes, heated at 1120 K for 70 h and quenched in water. Photoemission experiments were performed with several incident photon energies in the soft and hard x-ray regions at the end stations of SPring-8 (BL23SU, BL15XU and BL47XU). We used a photoemission spectrometer with a hemispherical photoelectron analyzer (SES2002/R-4000). The total-energy resolution was 100 meV at $h\nu = 765$ eV and 1090 eV (BL23SU), 150 meV at $h\nu = 5945$ eV (BL15XU), and

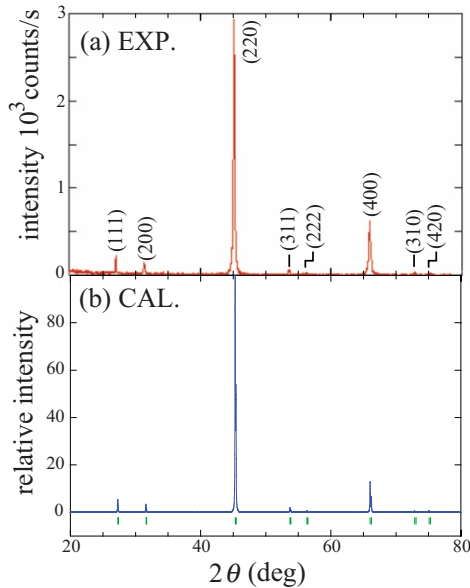


FIG. 1. (Color online) [(a) and (b)] The measured and simulated x-ray powder-diffraction patterns for Co_2MnSi .

280 meV at $h\nu=7935$ eV (BL47XU). All the measurements were done in an ultrahigh vacuum condition ($<6 \times 10^{-8}$ Pa). A clean surface was obtained by *in situ* fracturing of the sample.

We have also performed first-principles density-functional calculations using the Vienna *ab initio* simulation package^{18,19} within the spin-polarized generalized gradient approximation (GGA) using the Perdew-Becke-Ernzerhof parameterization²⁰ for the exchange and correlation energies. The nuclei and core electrons are described by the projector augmented plane-wave potential,^{21,22} and the wave functions are expanded in a plane-wave basis set with a cut-off energy of 337.3 eV. The Brillouin-zone integration is done with a modified tetrahedron method with Blöchl corrections²³ on the uniform $25 \times 25 \times 25$ mesh.

The structural property of the present sample has been characterized with x-ray powder-diffraction measurement at room temperature using Cu $K\alpha$ radiation. Figures 1(a) and 1(b) represent the observed and simulated x-ray diffraction patterns of Co_2MnSi , respectively. All the experimental diffraction lines can be indexed with the cubic structure with a lattice parameter $a=5.653$ Å. This value is in good agreement with those reported earlier.^{5,12–14} The strong sharp (220)-peak confirms the presence of a single cubic phase. The intensities of the superstructure lines such as (111) and (200) agree very well with the results calculated as the Heusler structure. This result ensures that the sample in this Rapid Communication has a fully ordered $L2_1$ structure.

The valence-band photoemission spectrum excited by hard x-ray ($h\nu \sim 6$ keV) synchrotron radiation at 30 K (open circles) near E_F is shown in the upper part of Fig. 2(a). The spectrum has several peak structures as denoted by A–E. The most intense peak (C) is observed at the binding energy (E_B) of 1.2 eV. The feature B at $E_B=0.7$ eV and a broad hump (E) at 2.7 eV are also recognized. These characteristic features are consistent with the reported spectra measured by the hard

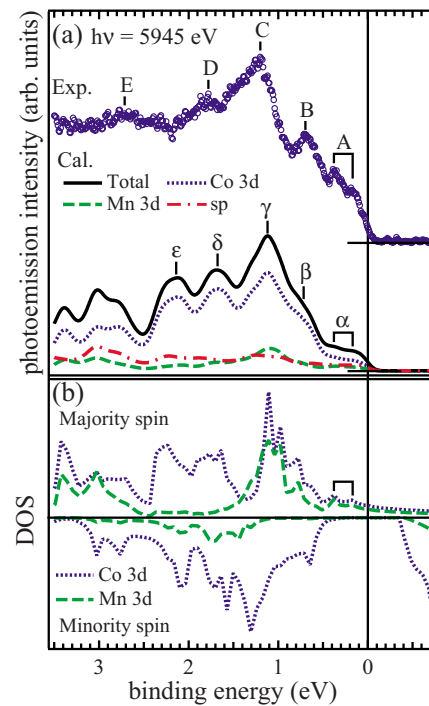


FIG. 2. (Color online) (a) Valence-band photoemission spectra excited by $h\nu=5945$ eV at low temperature (30 K) compared with simulated photoemission spectra using theoretical DOSs. Solid line exhibits the simulated total DOS, while dotted, dashed, and dash-dotted lines represent the simulated spectra contributed from the Co 3d, Mn 3d, and the *sp* electrons of constituent elements of Co_2MnSi . (b) Calculated majority- and minority-spin partial DOSs of Co 3d (dotted) and Mn 3d (dashed) states (see text).

x-ray photons (~ 6 and 8 keV).^{8,10} The improved energy resolution and high-flux photons of the present study enable us to observe two more characteristic features, A and D, which were not recognized in the previous reports.^{8,10} The structure A shows a double peak at 0.2 and 0.4 eV from E_F , and the single structure D is located at $E_B=1.8$ eV. The *sp* electrons of all the constituent elements of Co_2MnSi make a considerable contribution to the hard x-ray photoemission spectrum due to large photoionization cross section compared with that of *d* electrons.^{16,17} However, since the photoemission intensities taken at $h\nu=765$ eV in the E_B range from E_F to 2 eV are enhanced compared with those taken at $h\nu=7935$ eV (not shown), the Co 3d contribution is dominant in this binding-energy region. In the bottom of Fig. 2(a), we present calculated photoemission spectrum in which the photoionization cross sections for constituent elements, Fermi distribution function, and instrumental energy resolution have been taken into account. In the simulated photoemission spectrum, the solid lines exhibit the total spectral intensity, which is composed of partial DOSs of Co 3d, Mn 3d, and *sp* electrons of all elements as denoted by the dotted, dashed, and dash-dotted lines. The calculated photoemission spectrum has the structures denoted as α , β , γ , δ , and ϵ in the E_B range from E_F to 2.5 eV. Moreover, one recognizes that the Co 3d electrons also dominate the simulated photoemission spectrum in the E_B range of 0–2 eV as discussed above.

Here, the observed hard x-ray photoemission spectrum is compared with the calculated photoemission spectrum. The observed spectrum is consistent with the calculated one except for the slight differences in energy position and spectral weight. For example, the structure C in the experimental spectrum can be reasonably ascribed to γ with the largest weight although the peak of C is located at a 0.1 eV higher E_B than that of the calculated peak γ . Moreover, the structures B, D, and E in the experimental spectrum correspond to the structures β , δ , and ϵ in the calculated spectrum. Here we need to consider the recoil effect, that is the binding energy shift and linewidth broadening.²⁴ It is sizable in the photoemission spectra especially for the light elements such as carbon and boron.^{24,25} We have confirmed that the Si 2s core-level photoemission spectrum for $h\nu=7935$ eV shows negligible energy shift as well as no remarkable linewidth broadening in comparison with the spectrum for the reduced photon energy of 1090 eV (not shown). Therefore, the recoil effect should be negligible in the present work.

For a better understanding of the electronic states, the spin-dependent partial DOSs of Co and Mn 3d states are depicted in Fig. 2(b). Here, the majority- and minority-spin DOSs are shown in the upper and lower panels, respectively. It is easily recognized that the most intense feature γ comes from both majority- and minority-spin Co 3d DOSs with sharp peaks at $E_B=1.0$ and 1.3 eV, respectively. The majority-spin Co 3d state around $E_B=1$ eV is hybridized with the Mn 3d state, whereas the hybridization is weak for the minority-spin Co 3d state at $E_B=1.3$ eV. The discrepancy in the magnitudes between experimental and theoretical spectra might be partly caused by the different photoionization cross sections from atomic values, which could be modified by the different symmetry and spin of the same orbital and atom. It is noted that there are two peaks at $E_B=0.2$ and 0.4 eV in the calculated majority-spin DOS which exist in the energy gap of minority-spin DOS. This is in excellent agreement with the structure of A in the photoemission spectrum indicating the validity of the present band-structure calculation.

Finally, let us discuss the temperature dependence of the valence-band spectrum. Figure 3 shows the valence-band photoemission spectra measured at 30 K (open circles) and at 300 K (solid line). Here, the observed photoemission spectra at low and high temperatures can be compared with the DOS of DMFT calculation reported by Chioncel *et al.*⁷ at 0, 200, and 400 K. The result of the DMFT calculation predicts that the nonquasiparticle state grows in the minority-spin energy gap at E_F at finite temperatures. The predicted change in minority-spin DOS is too small to be observed due to the limited energy resolution in the present experiment. The calculation also predicts marked temperature dependence of the majority-spin DOS located at $E_B\sim 1$ eV, that is, the peak at $E_B\sim 1$ eV at 0 K shifts to lower energy by 250 meV at 400 K, which can be observed in this experiment if it is the case. However, our result clearly indicates that the photoemission spectra taken at 30 and 300 K are almost identical. The binding-energy shift of 250 meV of the peak C does not exist. This result indicates that the nonquasiparticle state might not be the main driving force for the reduced spin polarization at the increased tempera-

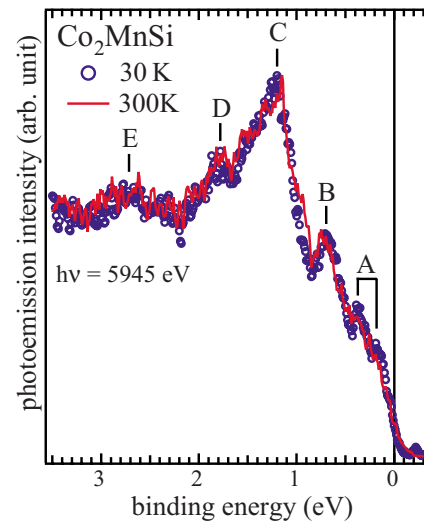


FIG. 3. (Color online) Valence-band photoemission spectra excited by $h\nu=5945$ eV at low temperature (30 K) and room temperature (300 K). Open circles and solid lines represent the spectra measured at low and room temperatures, respectively.

ture. The origin of the seriously reduced TMR ratio might be dominated by a spin mixing such as magnon excitations and inelastic scattering through interface states if the interface states between Co_2MnSi and the insulator sheet lose the minority-spin gap, as predicted by Marvopoulos *et al.*²⁶ Actually, the first-principles calculation for $\text{Co}_2\text{MnSi}/\text{MgO}/\text{Co}_2\text{MnSi}$ has predicted that the interface states lose spin polarization at E_F , while the half metallicity is preserved only a few atomic layers away from the interface.^{27,28} From a recent experimental report with hard x-ray photoemission, the overall features of the valence-band spectrum of a Co_2MnSi film buried under the MgO barrier was similar to that of bulk.¹⁰ However, it is still questionable if a few atomic layers from the interface can be sufficiently resolved from previous experiment with an enhanced photoelectron escape depth (~ 170 Å). Further investigation with high-resolution spin-resolved spectroscopy is required to reveal the interface electronic states.

In summary, the electronic structure of full Heusler-type alloy Co_2MnSi has been studied by the soft and hard x-ray photoemission spectroscopies. The observed photoemission spectra are in qualitative agreement with the result of band-structure calculations based on the GGA scheme. No significant difference has been observed between the valence-band photoemission spectra at 30 and at 300 K at variance with the significant temperature-dependent modification of the DOS predicted by the DMFT calculation. Present results require re-examination of the explanation based on the DMFT calculation. We have discussed spin mixing in the presence of interface as an alternative explanation.

The synchrotron radiation experiments were performed at SPring-8 with the approvals of JASRI (Grant No. 2006B1604/BL47XU) as Nanotechnology Support Project of the MEXT, JAEA (Grant No. 2006B3815/BL23SU), and NIMS (Grant No. 2008A4802/BL15XU). We acknowledge Y. Yamashita and H. Yoshikawa of NIMS and S. -i. Fujimori

of JAEA for their technical support during the experiment. The analyzer development at BL47XU was supported by SENTAN, Japan Science and Technology Agency. This work was partially supported by the Ministry of Education, Culture, Sports, Science, and Technology of Japan through a

Grant-in-Aid for Scientific Research (B) (Grant No. 17340112) and for Scientific Research in Priority Area “Creation and Control of Spin Current” (Grant No. 1904802) and a Cooperative Research Project Program of RIEC, Tohoku University.

-
- ¹R. A. de Groot, F. M. Mueller, P. G. van Engen, and K. H. J. Buschow, *Phys. Rev. Lett.* **50**, 2024 (1983).
- ²G. A. de Wijs and R. A. de Groot, *Phys. Rev. B* **64**, 020402(R) (2001).
- ³S. Ishida, S. Fujii, S. Kashiwagi, and S. Asano, *J. Phys. Soc. Jpn.* **64**, 2152 (1995).
- ⁴S. Ishida, T. Masaki, S. Fujii, and S. Asano, *Physica B* **245**, 1 (1998).
- ⁵P. J. Webster, *J. Phys. Chem. Solids* **32**, 1221 (1971).
- ⁶Y. Sakuraba, M. Hattori, M. Oogane, Y. Ando, H. Kato, A. Sakuma, T. Miyazaki, and H. Kubota, *Appl. Phys. Lett.* **88**, 192508 (2006).
- ⁷L. Chioncel, Y. Sakuraba, E. Arrigoni, M. I. Katsnelson, M. Oogane, Y. Ando, E. Burzo, T. Miyazaki, and A. I. Lichtenstein, *Phys. Rev. Lett.* **100**, 086402 (2008).
- ⁸B. Balke, G. H. Fecher, H. C. Kandpal, C. Felser, K. Kobayashi, E. Ikenaga, J. J. Kim, and S. Ueda, *Phys. Rev. B* **74**, 104405 (2006).
- ⁹W. H. Wang, M. Przybylski, W. Kuch, L. I. Chelaru, J. Wang, Y. F. Lu, J. Barthel, H. L. Meyerheim, and J. Kirschner, *Phys. Rev. B* **71**, 144416 (2005).
- ¹⁰G. H. Fecher, B. Balke, A. Gloskowskii, S. Ouardi, C. Felser, T. Ishikawa, M. Yamamoto, Y. Yamashita, H. Yoshikawa, S. Ueda, and K. Kobayashi, *Appl. Phys. Lett.* **92**, 193513 (2008).
- ¹¹C. R. Brundle, *J. Vac. Sci. Technol.* **11**, 212 (1974).
- ¹²R. A. Dunlap and D. F. Jones, *Phys. Rev. B* **26**, 6013 (1982).
- ¹³P. J. Brown, K. U. Neumann, P. J. Webster, and K. R. A. Ziebeck, *J. Phys.: Condens. Matter* **12**, 1827 (2000).
- ¹⁴R. Y. Umetsu, K. Kobayashi, A. Fujita, R. Kainuma, and K. Ishida, *Scr. Mater.* **58**, 723 (2008).
- ¹⁵K. Kobayashi, M. Yabashi, Y. Takata, T. Tokushima, S. Shin, K. Tamasaku, D. Miwa, T. Ishikawa, H. Nohira, T. Hattori, Y. Sugita, O. Nakatsuka, A. Sakai, and S. Zaima, *Appl. Phys. Lett.* **83**, 1005 (2003).
- ¹⁶M. B. Trzhaskovskaya, V. I. Nefedov, and V. G. Yarzhevsky, *At. Data Nucl. Data Tables* **77**, 97 (2001).
- ¹⁷M. B. Trzhaskovskaya, V. I. Nefedov, and V. G. Yarzhevsky, *At. Data Nucl. Data Tables* **82**, 257 (2002).
- ¹⁸G. Kresse and J. Hafner, *Phys. Rev. B* **47**, 558 (1993).
- ¹⁹G. Kresse and J. Furthmüller, *Comput. Mater. Sci.* **6**, 15 (1996); *Phys. Rev. B* **54**, 11169 (1996).
- ²⁰J. P. Perdew, K. Burke, and M. Ernzerhof, *Phys. Rev. Lett.* **77**, 3865 (1996).
- ²¹P. E. Blöchl, *Phys. Rev. B* **50**, 17953 (1994).
- ²²G. Kresse and D. Joubert, *Phys. Rev. B* **59**, 1758 (1999).
- ²³P. E. Blöchl, O. Jepsen, and O. K. Andersen, *Phys. Rev. B* **49**, 16223 (1994).
- ²⁴Y. Takata, Y. Koyama, M. Yabashi, K. Tamasaku, Y. Nishino, D. Miwa, Y. Harada, K. Horiba, S. Shin, S. Tanaka, E. Ikenaga, K. Kobayashi, Y. Senba, H. Ohashi, and T. Ishikawa, *Phys. Rev. B* **75**, 233404 (2007).
- ²⁵S. Suga, *Appl. Phys. A: Mater. Sci. Process.* **92**, 479 (2008).
- ²⁶P. Mavropoulos, M. Lezaic, and S. Blugel, *Phys. Rev. B* **72**, 174428 (2005).
- ²⁷Y. Miura, H. Uchida, Y. Oba, K. Nagao, and M. Shirai, *J. Phys.: Condens. Matter* **19**, 365228 (2007).
- ²⁸Y. Miura, H. Uchida, Y. Oba, K. Abe, and M. Shirai, *Phys. Rev. B* **78**, 064416 (2008).